International Academic Institute for Science and Technology

International Academic Journal of Science and Engineering
Vol.11, No.1, 2024, pp.98-106.

ISSN 2454-3896

International Academic Journal of Science and Engineering

www.iaiest.com

Diagnosis of DC Glow Discharge Plasma of Krypton Gas Under Different Pressures

Mohammed H. Jawad [a], Zahraa T. Turki [b]

[a] *College of Pharmacy, Ahl Al Bayt University, Karbala, Iraq. E-mail: muhamedhamza99@abu.edu.iq*
[b] *College of Health and Medical Technologies, Department of Anesthesiology, University of Al Zahraa for Women, Karbala, Iraq. E-mail: zahraa.talib@alzahraa.edu.com*

Abstract

In this study, we looked at how various pressure levels affected the plasma produced by the krypton gas blazing electric discharge. Various pressure readings between 0.6 and 1.4 Torr were employed. At 300 K in temperature a three-dimensional computer simulation based on the krypton plasma finite element approach was executed. By acquiring the plasma parameters (electron density, electric potential, and electron temperature), we were able to obtain a higher density plasma based on our findings.

Keywords: Plasma Physics, COMSOL Multiphysics, Simulation.

DOI: 10.71086/IAJSE/V11I1/IAJSE1113
Received: 07 January 2024/Accepted: 20 February 2024/Published: 27 February 2024

Introduction

Whenever the electrons or photons in enough power hit with natural atomic and molecular in the source gas, they produce electron and ion in a gases phases. Plasma is created through adding power transformed into an unbiased gas, resulting in production of charges carrier [2,3]. The One kind of plasma known as glow discharge is described as the partially ionized gas with a high concentration of neutral species and roughly equal concentrations of positive and negative charges. An inert or molecular gas filled under minimal pressures cell produces the glow discharge [4]. The glow discharge plasma is produced by applying a potential difference between two electrodes, which can either be placed inside a cell or serve as the cell walls. In fact, the process known as "gas breakdown" occurs when discharge gas atoms ionize due to the potential difference, producing positively charged ions and free electrons [5,6]. The electrons that are released by the positive ions as they accelerate towards the cathode of the glow discharge are known as secondary electron emission. Once in the plasma, the electrons can cause collisions with the gas particles, the most significant of which excite and ionize the gas particles [7,8]. This study examined the characteristics of argon plasma produced by electrostatic discharge using aluminum as the electrode target. To find plasma properties like electron temperature (Te) and electron number density (ne), run a two-dimensional simulation for various voltage levels using the Comsol tool.

Modeling of Glow Discharge Plasma

Equations of drift are solved to obtain electrons density and energies, as shown below. A Poisson equation which shows an equilibrium between positive ions and electrons in the particle density, provides a mathematical explanation for the DC light discharge [9].

$$-\nabla.\epsilon_0\epsilon_r\nabla V = \rho \quad (1)$$

$$\frac{\partial(n_e)}{\partial t} + \nabla.[-n_e(\mu e.E) - De.\nabla ne] = Re \quad (2)$$

$$\frac{\partial(n_\varepsilon)}{\partial t} + \nabla.[-n_\varepsilon(\mu_\varepsilon.E) - D_\varepsilon.\nabla n_\varepsilon] + (E.\Gamma_\varepsilon) = R_\varepsilon \quad (3)$$

$$\Gamma_\varepsilon = -n_e(\mu e.E) - De.\nabla ne \quad (4)$$

The energy loss R_ε, from elastic collisions and the R_e electron source will be specified. The formulae below will be used to compute electron and energy diffusion, as well as energy mobility.

$$D_\varepsilon = \mu e\, T_e\,,\ \mu_\varepsilon = \left(\frac{5}{3}\right)\mu e, D_\varepsilon = \mu_\varepsilon T_e \quad (5)$$

Source coefficients in plasma chemistry equations that assume the number of interactions (M) in some neutral inelastic collisions (P) to be the number of interactions where in general P >> M. The source of the electron according to rate coefficients is obtained through the following relationship.

$$Re = \sum_{(j=1)}^{(M)} X_j\, K_j N_n n_e \quad (6)$$

xj A target species' mole fraction in response j, k_j is the reaction j rate coefficients (m^3/s), (N_n) overall neutral numbers intensity ($1/m^3$). It is more efficient to apply Rate coefficients are replaced with Townsend parameters. when defining reaction rates. Townsend coefficients help us understand the occurrences in the cathode sinking zone better; the electrons sources is provided.

$$R_e = \sum_{j=1}^{M} X_j\, \alpha_j N_n |\Gamma_e| \quad (7)$$

Townsend's coefficient is (αj). Numerical computations are made more stable by the Townsend coefficients. Electron energy is lost as a result of the reaction's cumulative collision-related energy loss.

$$R_\varepsilon = \sum_{j=1}^{P} X_j\, K_j N_n n_e \Delta\varepsilon_j \quad (8)$$

Where $\Delta\varepsilon_j$ is how much energy is lost during a response j. The rate coefficients are computed using the following integral and the cross-section data. Each non-electronic type's mass fraction is determined by:

$$\rho = q\int_{\infty}^{0} \varepsilon\, \sigma_k\,(\varepsilon) f(\varepsilon) d\varepsilon \quad (9)$$

$$R_\varepsilon = \sum_{j=1}^{P} X_j\, K_j \alpha_j N_n |\Gamma_e| \Delta_{\varepsilon j} \quad (10)$$

The mass fraction of every non-electron species is found using the following equation:

$$\rho = \frac{\partial}{\partial t} w_k - \rho(u.\nabla) w_k = \nabla . j_k + R_k \quad (11)$$

In this model, a density of space charges is computed using plasma chemistry [9].

$$\rho = q \sum_{K=1}^{N} Z_j n_k - n_e \quad (12)$$

[6].

Geometry and Mesh

This research simulates the (DC) glow discharge in a system of planar electrodes in two dimensions, like depicted within the figure in a 40 cm long discharging mechanism. As shown in Fig. 1, while being affected by varying voltage values (125V, 145V, 165V, and 185V) and a pressure of 0.6 torr. This allowed us to solve the proposed model using the finite element approach in the simulation with less time and effort. The distance where the network elements have just been put along the negative electrode and positive electrode is known as the solution area. Most significant occurrences take place in this range.

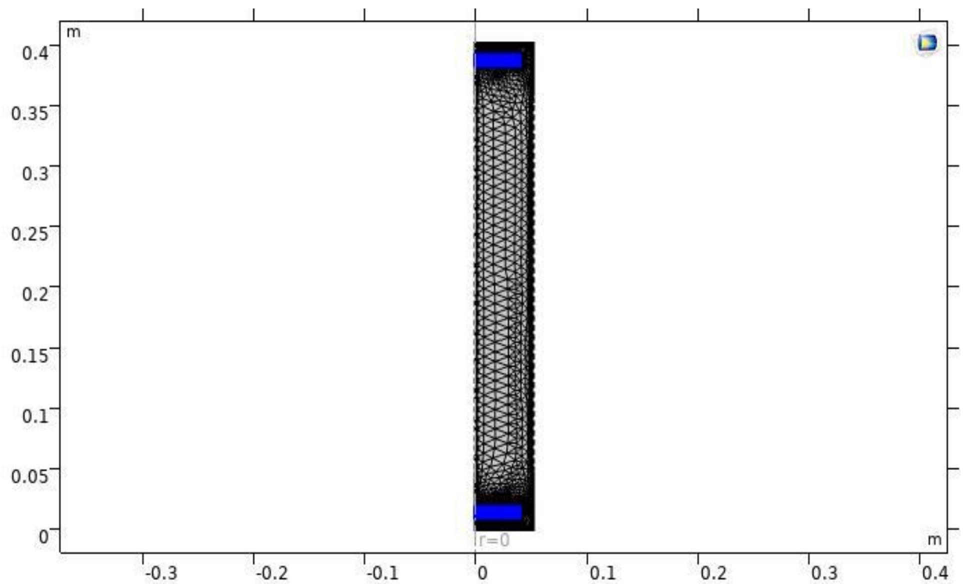

Figure 1: The Geometry of the Electrodes and Mesh Solution

Chemical Reactions of Krypton Gas

Table 1, which lists the various cross-sectional energies of the ionization, excitation, and elasticity processes that occur in argon plasma, Table 2 shows the surface reaction of argon, which is also referred for as acoustic responses. A likelihood that an atom will revert to its initial condition after colliding with a wall is shown by the adhesion coefficient in Table 2. Gas reaction cross-sectional derived from LXCAT [10].

Table 1: Krypton Gas Reactions and Collision [12]

Interactive formula		type	(Δε (eV))
1	kr +e ≥ e +kr	Elastic	0
2	kr + e ≥ krs + e	Excitation	11.5
3	krs + e ≥ kr + e	Superelastic	-11.5
4	kr + e ≥ kr^+ + 2e	Ionization	15.8
5	krs + e ≥ kr^+ + 2e	Ionization	4.24
6	krs+ krs≥ kr^++kr+e	Penning Ionization	-
7	kr + krs ≥ kr + kr	Metastable quenching	-

Table 2: Reaction of Argon Gas and Collision [12]

Interactive formula		Adhesion factor
1	krs ≥ kr	1
2	kr^{+} ≥ kr	1

The Results and Discussion

A simulation conducted in two dimensions of the DC glow discharge plasma was performed with a Comsol Multiphysics software. A separate ring with (resistance R) with (capacitor C) linked in tandem with the release provides a positive voltage to the anode, provided that the cathode is grounded. The outcomes that were attained were as follows.

Electron Density

The characteristics and attributes of the resultant plasma are determined by the electron density. In this model, it was computed using the solution of two equations related to Density of electrons, mean scatter with drifting. (Fig.2) reveals the electrons intensity distribution at the discharging technique's center. It had been observed the most electrons rush towards the anode region when the discharge system's voltage is applied increases. This is because the strong electric field accelerates the electrons in the anode region, increasing their density, which peak inside the area between the column that is positive and the cathode glow. Figure 3 provides further clarification by showing the electron density distribution in the path that joins the two electrodes. The results were in agreement with experimental investigations, such as the researcher's and others' study, which established that fact [11].

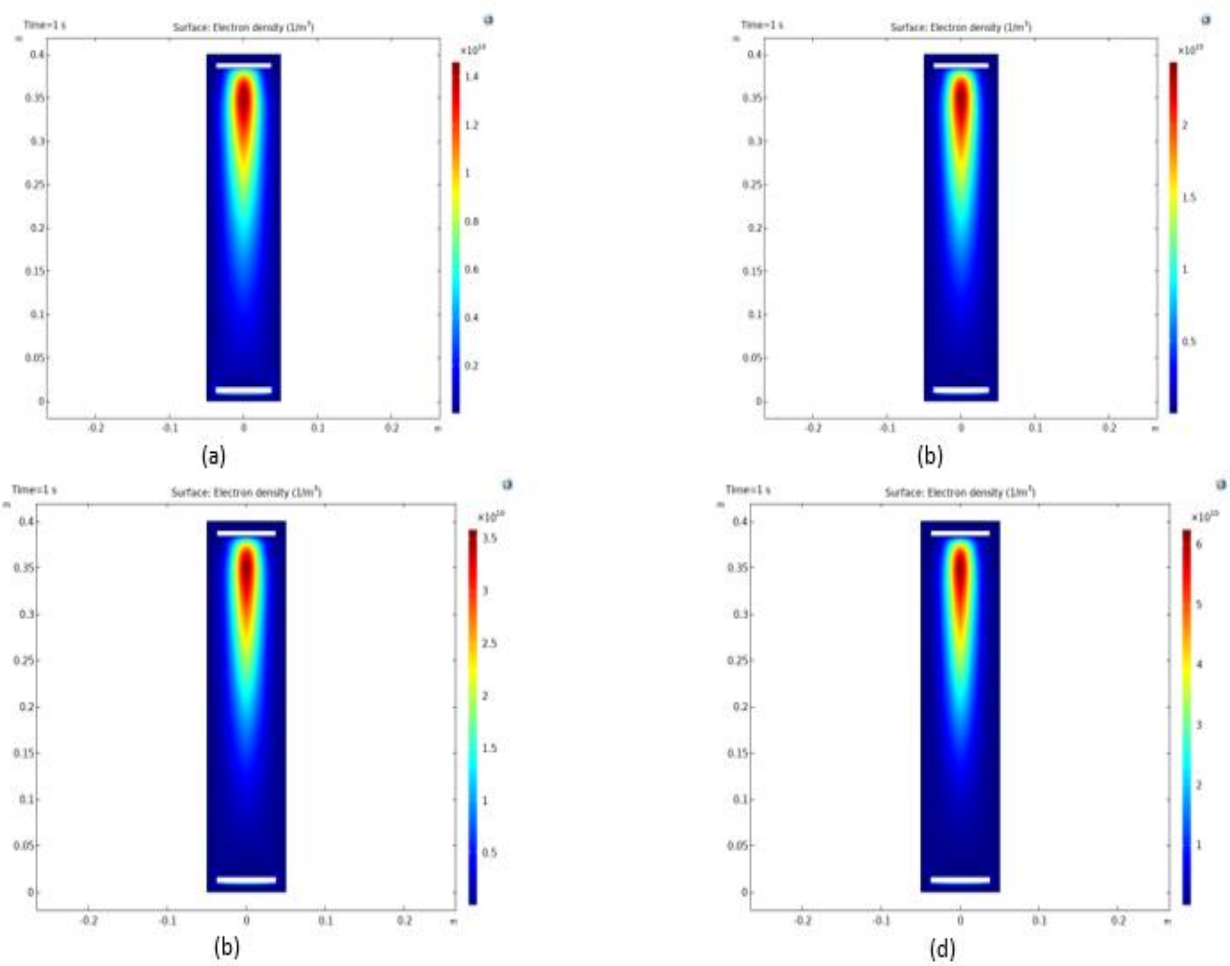

Figure 2: At the Center of the Tube, The Distribution of Electron Density with Respect to Axial Length at Various Pressure: (a) 0.6, (b) 0.8, (c) 1, (d) 1.4

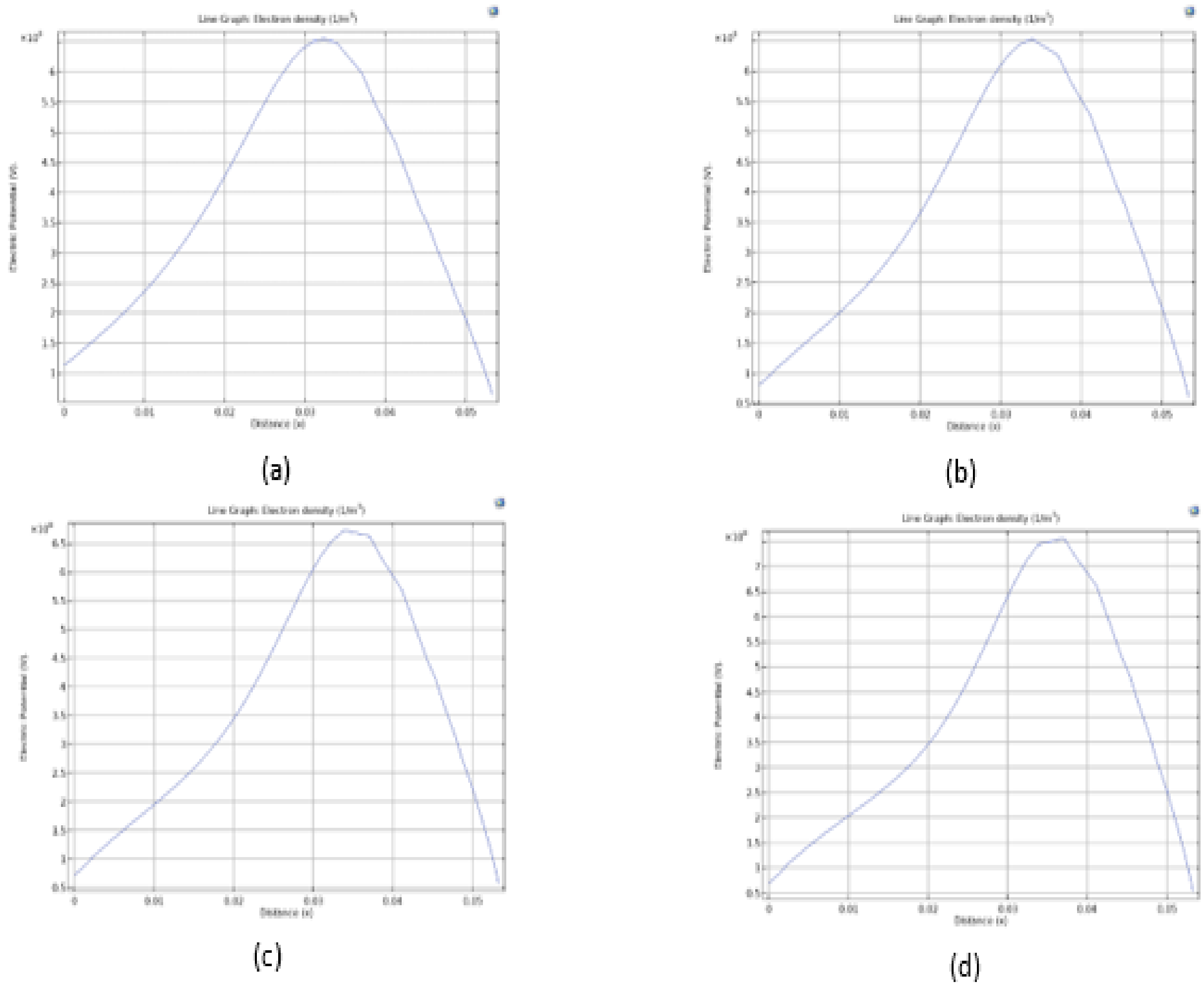

Figure 3: Electron Density's Spatial Contour at Different Pressures.

a) 0.6 torr, b) 0.8 torr, c) 1torr, d) 1.4 torr

Electron Temperature

A crucial element in defining the characteristics and parameters of the resultant plasma is the temperatures of electrons. The (argon gas) plasmas electron temperature it evaluated while 0.5 torr of pressure and 125, 145, 165, and 185 V of voltage were applied. Figure 4 illustrates how an increase in voltage causes an electron's temperature to rise as it seens to be dispersed With the cathode's sparkle, horizontally zone. To provide further context, let me explain. In figure 5, this diagram made in the same direction that separates positive and negatives electrodes. This was done after it was discovered that a strong electric field in the cathode region can attract high energy ion, which The positive electrode will warm up and become release heated electrons increase in number as released toward its outermost part. After ions attack cathode, a peak electron temperature is reached and kinematic energy-rich additional electrons are emitted, leading to a rapid drift speed along a cathode's darkness area section columnar. These findings were in line with experimental investigations, such as the researcher's and others' study, which established this fact [12].

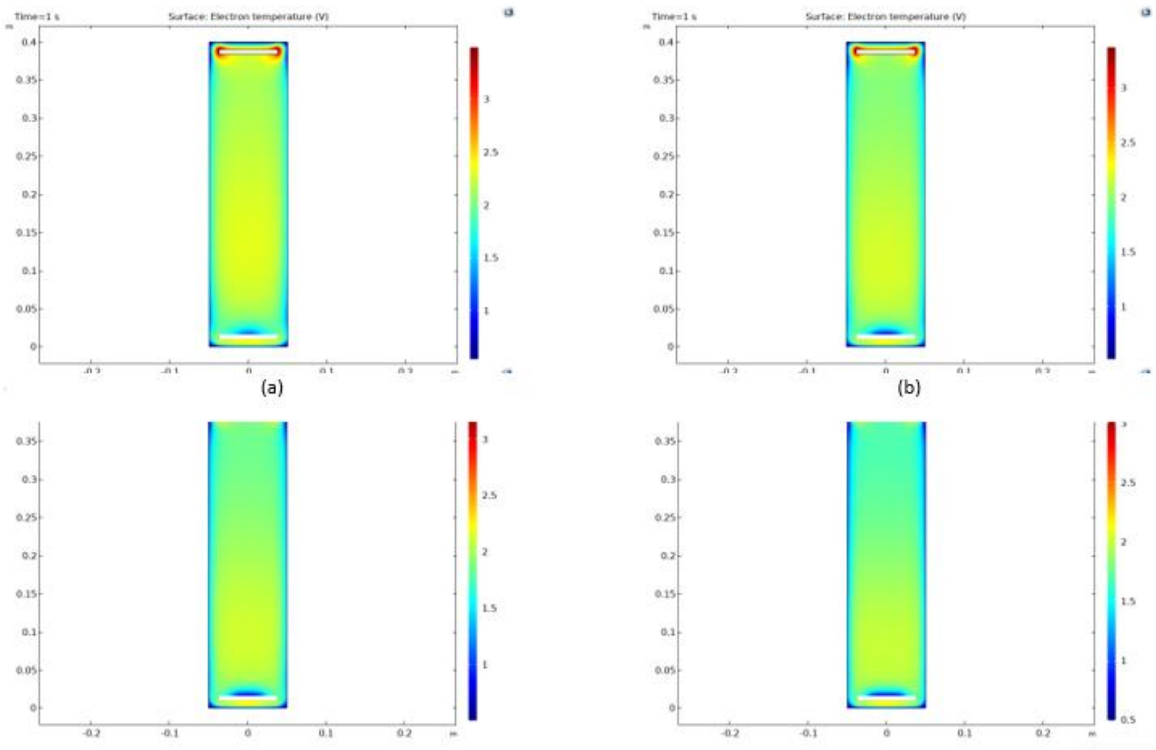

Figure 4: Distribution of Electron Temperature in Relation to Axial Length at the Tube's Core at Various Pressure: a) 0.6 torr, b) 0.8 torr, c) 1torr, d) 1.4 torr

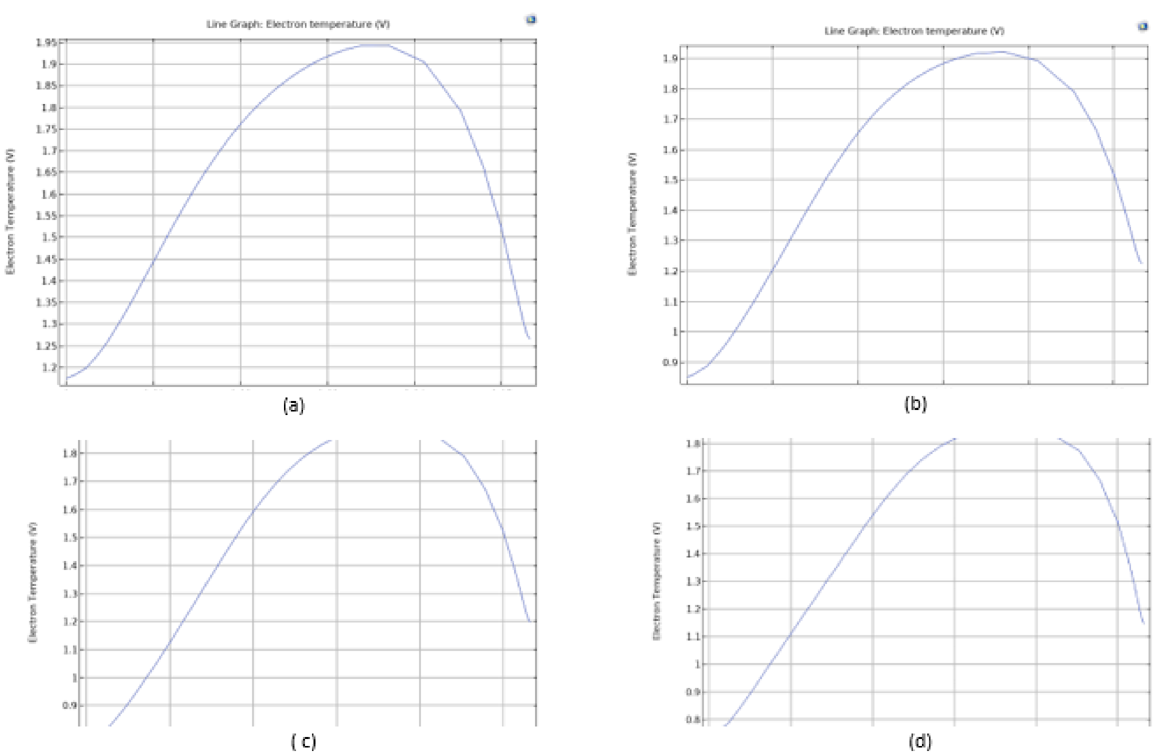

Figure 5: The Spatial Profile of Electron Temperature at Various Pressure a) 0.6 Torr, b) 0.8 Torr, c) 1 Torr, d) 1.4 Torr

Electric Potential

Figure 6 shows the distribution of the external argon voltage against the axis length when 0.5 torr of pressure and 125, 145, 165, and 185 V of voltage were applied. It has been noted that when voltage rises, so does electric potential. An ion concentration at the cathode fall zone is significantly more of that of electron, is depicted in figure. The peaks voltages in this region indicates that the build-up of charged particle, mainly ion, are main cause of the electrical conductivity decrease in this area. This findings was in line utilizing unorthodox investigations, such as the researcher's and others' study, which established this to be the case [13].

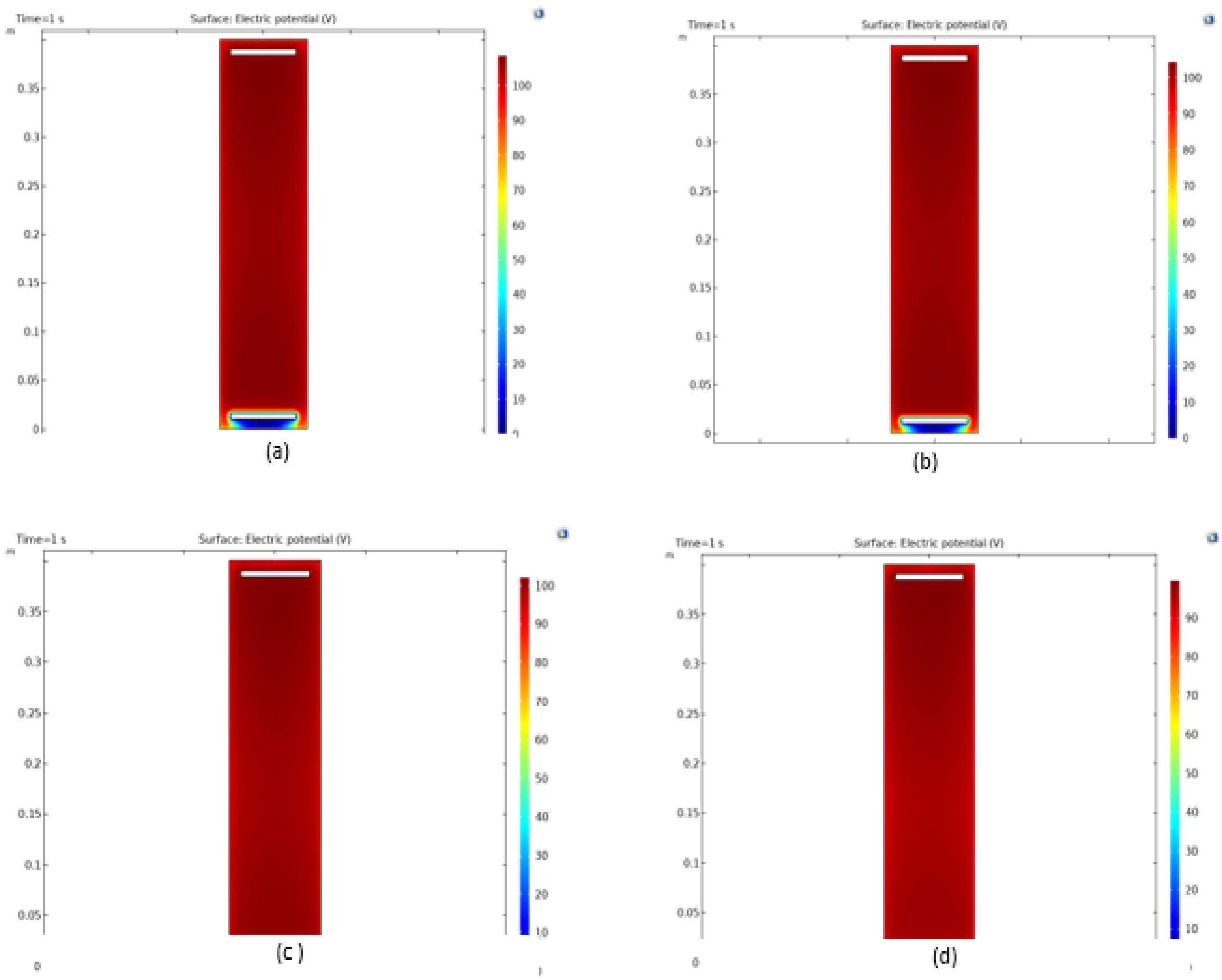

Figure 6: Distribution of Electric Potential in Relation to Axial Length at the Tube's Core, at Various Pressure: a) 0.6 Torr, b) 0.8 Torr, c) 1 Torr, d) 1.4 Torr

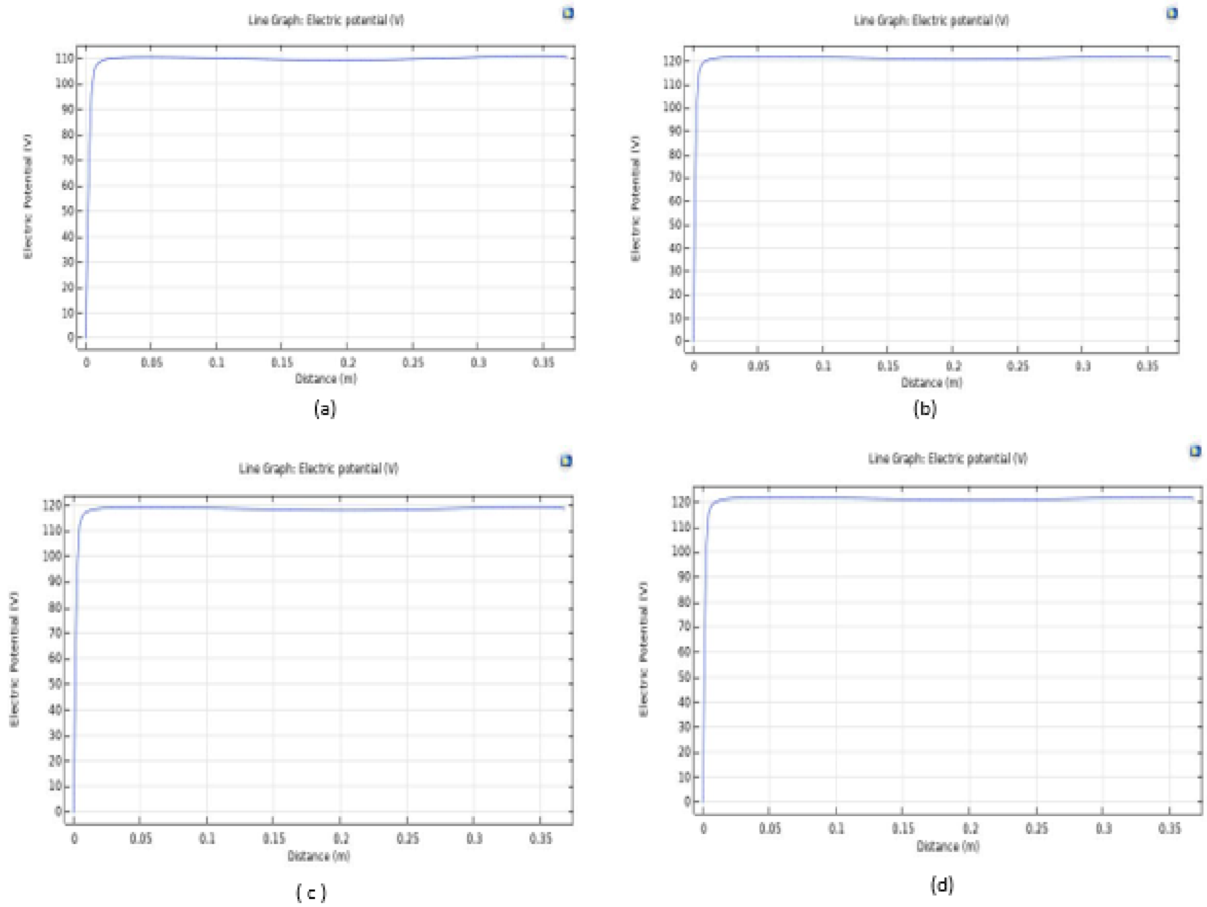

Figure 7: The Spatial Profile of Electric Potential at Various Voltages

a) 0.6 Torr, b) 0.8 Torr, c) 1 Torr, d) 1.4 Torr

Conclusions

In order to study the plasma resulting from the glow discharge of krypton gas, three-dimensional numerical simulations were used using the Comsol program at a constant voltage value of 125 volts and a gas temperature of 300 K. There were different voltage values (0.6, 0.8, 1, 1.4 Torr), as the electrode material was made of copper. The results showed that the resultant plasma is densely packed at the pressures used, and being a definite outcome pressure on the characteristics of the generated plasma. It was discovered that the temperature also density of electron and an electrical voltage increase with increasing values of the applied voltages.

References

Almeida, P.G.C., & Benilov, M.S. (2011). Modelling DC glow discharges in a wide range of currents with COMSOL Multiphysics. New results, fortes and weaknesses. *In Proc. 30th Int. Conf. Phenomena in Ionized Gases, Belfast, United Kingdom*.

Yahya, K.A., & Rasheed, B.F. (2016). Effect of Electrodes Separation in DC Plasma Sputtering on Morphology of Silver Coated Samples. *Al-Nahrain Journal of Science*, *19*(4), 78-85.

Kelly, P.J., & Arnell, R.D. (2000). Magnetron sputtering: a review of recent developments and applications. *Vacuum*, *56*(3), 159-172.

Almeida, P.G., Benilov, M.S., & Faria, M.J. (2010). Multiple solutions in the theory of dc glow discharges. *Plasma Sources Science and Technology*, *19*(2), 025019.

Gudmundsson, J.T., & Hecimovic, A. (2017). Foundations of DC plasma sources. *Plasma Sources Science and Technology*, *26(12),*123001. https://doi.org/10.1088/1361-6595/aa940d

Aadim, K.A., & Yousef, A.A. (2018). Spectroscopic study of AL nitrogen plasma produced by DC glow discharge. *Iraqi Journal of Science*, 494-501.

Rafatov, İ., & Kudryavtsev, A. (2012). On the numerical modelling of a dc driven glow discharge plasma. https://hdl.handle.net/11511/75507

Kadhim, M. M., Abbas, Q.A., & Abdulameer, M.R. (2022). Study of some plasma characteristics in dielectric barrier discharge (DBD) system. *Iraqi Journal of Science*, 2048-2056.

Schmitt, W., Köhler, W.E., & Ruder, H. (1992). A one-dimensional model of dc glow discharges. *Journal of applied physics*, *71*(12), 5783-5791.

Cross section extracted from (www.lxcat.net)

Jha, V.K., Mishra, L.N., & Narayan, B. (2017). Effect of Pressure and Discharge Voltage on Plasma Parameters in Air seeded Arc-plasma. *Physics and Astronomy Research*, *3*, 74-78.

Somayajula, S.K., Sriram, A.T., & Shelar, V.M. (2020). Study of Argon and Xenon gas properties on DC-glow discharge plasma. In *Journal of Physics: Conference Series*, *1706*(1).

Jawad, M.H., & Abdulameer, M.R. (2023). The effect of background argon gas pressure on parameters of plasma produced by Dc-glow discharge. *Iraqi Journal of Science*, 1210-1218.